ELSEVIER

Chemical Engineering Journal 85 (2002) 215–223

Chemical Engineering Journal

www.elsevier.com/locate/cej

A numerical study of flow and mixing characteristics of laminar confined impinging streams

Sakamon Devahastin [a,*], Arun S. Mujumdar [b,1]

[a] *Department of Chemical Engineering, McGill University, 3610 University Street, Montreal, Que., Canada H3A 2B2*
[b] *Department of Mechanical Engineering, National University of Singapore, 10 Kent Ridge Crescent, Singapore 119260, Singapore*

Received 30 June 2000; received in revised form 28 February 2001; accepted 12 March 2001

Abstract

Numerical simulations were performed to study the flow and mixing characteristics of two-dimensional laminar confined impinging streams. By solving the time-dependent conservation equations for mass, momentum and energy, Reynolds numbers beyond which the flow becomes oscillatory and even random were determined for different geometric configurations. Simulations were also performed for cases with jet Reynolds numbers in the stable regime to study the mixing characteristics of the system. It is found that both the inlet jet Reynolds number and the geometry of the system have strong effects on mixing in impinging streams.

Keywords: Flow regime diagram; In-line mixer; Onset of instability; Opposing jets

1. Introduction

Impinging streams (IS) constitute a new class of flow configuration which has proved useful in conducting a wide array of chemical engineering unit operations, e.g. absorption, drying, mixing. Although a number of publications have reported uses of impinging streams in various applications [1–8], very few papers [9–13] are focused on studies of the fundamental transport processes in this flow configuration even in the laminar flow regime which is of practical importance when dealing with high viscosity fluids, e.g. polymer solutions, polymer melts, liquid foodstuffs, etc.

Although a number of works have been devoted to the study of confined impinging jets at low Reynolds number [14], little is reported about the flow and thermal characteristics of confined impinging streams (or opposing jets). Roy et al. [15] studied, both numerically and experimentally, laminar steady two-dimensional mixing flow in a junction (one-way exit impinging streams). By using a laser Doppler velocimeter (LDV) they were able to obtain the transition Reynolds number (based on the mean velocity in the exit branch) beyond which the flow in the exit branch becomes turbulent. This result will be discussed further in a subsequent section.

Hosseinalipour and Mujumdar [12] used temperature as a passive tracer to monitor mixing of two fluid streams of different temperatures in their numerical study of flow and thermal characteristics of steady two-dimensional confined laminar opposing jets. They found that by increasing the jet Reynolds number the attainment of uniformity of the temperature profile (and hence complete mixing of the two streams) is delayed. This is attributed to the shorter residence time of the fluid in the system due to the increased mean flow rate.

In the present study, time-dependent conservation equations for mass, momentum and energy were solved to obtain the flow characteristics of a two-dimensional laminar confined impinging stream geometry (Fig. 1). The Reynolds numbers (based on inlet jet hydraulic diameter) beyond which the flow displays periodicity and in some cases randomly fluctuates were identified for different geometric configurations. It is found that this transition Reynolds number depends strongly on the geometric parameter, viz. the ratio of the height of the exit channel to the width of the inlet jet, especially at lower values of this ratio.

Simulations were also performed for cases with jet Reynolds numbers in the stable regime to study the mixing characteristics of the system. The effects of inlet jet Reynolds number and geometric configuration on the mixing are studied and discussed.

* Corresponding author. Tel.: +1-514-398-4494; fax: +1-514-398-6678.
E-mail address: sdevah@po-box.mcgill.ca (S. Devahastin).
[1] Formerly at the Department of Chemical Engineering, McGill University, Montreal, Que., Canada.

1385-8947/02/$ – see front matter
PII: S1385-8947(01)00163-2

Nomenclature

c_p	heat capacity ($J\,kg^{-1}\,K^{-1}$)
D_h	inlet channel hydraulic diameter (m)
g_i	gravitational force vector ($m\,s^{-2}$)
H	height of the exit channel (fixed at 0.01 m)
k	thermal conductivity ($W\,m^{-1}\,K^{-1}$)
L	length of the exit channel (m)
p	pressure (Pa)
t	time (s)
T	temperature (°C)
ΔT	temperature difference of the two inlet streams (°C)
u	velocity component in x-direction ($m\,s^{-1}$)
u_i, u_j	velocity components ($m\,s^{-1}$)
v	velocity component in y-direction ($m\,s^{-1}$)
v_j	jet velocity ($m\,s^{-1}$)
V	dimensionless velocity component in y-direction ($V = v/v_j$)
W	width of the inlet channel (m)
x_i, x_j	coordinate (m)

Greek letters

μ	dynamic viscosity ($kg\,m^{-1}\,s^{-1}$)
ρ	density ($kg\,m^{-3}$)
σ_T	standard deviation of temperature (°C)
Θ	dimensionless time ($\Theta = tW/v_j$)

Dimensionless group

Re_j	jet Reynolds number ($D_h v_j \rho/\mu$)

2. Mathematical formulation

To formulate the mathematical description of the transport processes in impinging streams the following assumptions are made: the flow is laminar, incompressible and the fluid is Newtonian with constant physical properties. Viscous dissipation is neglected. The flow is assumed to be fully developed (both hydrodynamically and thermally) at the exit of the IS.

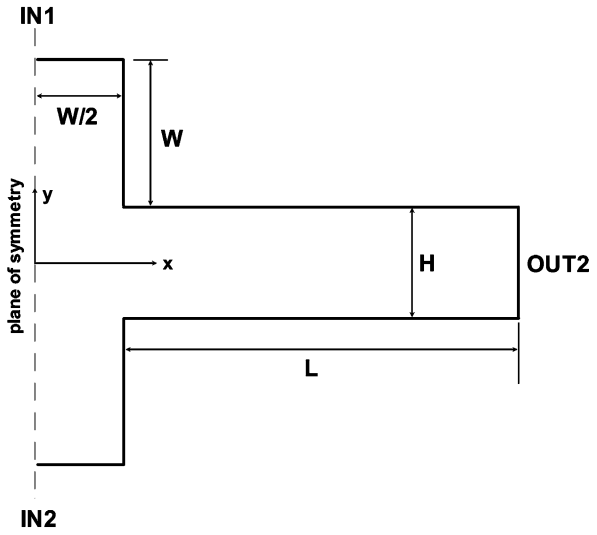

Fig. 1. Schematic diagram of the impinging streams studied.

Based on the above assumptions, conservation equations for mass, momentum and energy (in tensor form) can be written as follows [16]:

Continuity equation:

$$\frac{\partial u_i}{\partial x_i} = 0 \tag{1}$$

Momentum equation:

$$\rho\left(\frac{\partial u_j}{\partial t} + u_i\frac{\partial u_j}{\partial x_i}\right) = -\frac{\partial p}{\partial x_j} + \mu\frac{\partial}{\partial x_i}\left(\frac{\partial u_j}{\partial x_i}\right) + \rho g_j \tag{2}$$

Energy equation:

$$\rho c_p\left(\frac{\partial T}{\partial t} + u_i\frac{\partial T}{\partial x_i}\right) = k\frac{\partial}{\partial x_i}\left(\frac{\partial T}{\partial x_i}\right) \tag{3}$$

in which i and j take on the values 1 and 2.

These equations were solved numerically subject to the following initial and boundary conditions (see Fig. 1 for the description of symbols used):

Initial conditions:

$$\text{At } t = 0, \quad u_i = 0 \text{ and } T = 20^\circ\text{C} \tag{4}$$

Boundary conditions:

Inlet 1:

$$\left(0 < x < \tfrac{1}{2}W;\ y = W + \tfrac{1}{2}H\right)$$
$$u_1 = 0;\ u_2 = -u_{2,\text{jet}} \text{ and } T = T_{\text{inlet 1}} \tag{5}$$

Inlet 2:

$$\left(0 < x < \tfrac{1}{2}W;\ y = -\left(W + \tfrac{1}{2}H\right)\right)$$
$$u_1 = 0;\ u_2 = u_{2,\text{jet}} \text{ and } T = T_{\text{inlet 2}} \tag{6}$$

Top and bottom walls:

$$\left(\frac{W}{2} < x < L + \frac{W}{2}\right) \quad u_i = 0 \text{ and } \frac{\partial T}{\partial y} = 0 \tag{7}$$

Outlet:

$$\left(x = L + \tfrac{1}{2}W\right) \quad \frac{\partial \phi}{\partial x} = 0 \tag{8}$$

Along the symmetrical plane:

$$(x = 0) \quad \frac{\partial \phi}{\partial x} = 0 \tag{9}$$

where ϕ represents all solved variables.

The conservation equations, along with the initial and boundary conditions, were solved numerically using control-volume-based computational fluid dynamic software PHOENICS Version 2.2.2 [17]. In this code the convection terms in the momentum and energy equations were

discretized using the hybrid scheme [18]. A fully implicit scheme [18] was used to discretize the transient terms. The discretized equations were solved using the well-known SIMPLEST algorithm [17]. The solution was considered converged when the following criterion has been met for all dependent variables:

$$\max \left| \frac{\phi^{n+1} - \phi^n}{\phi_r} \right| \leq 10^{-3} \quad (10)$$

between sweeps n and $n+1$; ϕ_r represents the reference value for the dependent variable ϕ. To improve convergence under-relaxation of the false transient type was used for the two velocity components and the temperature. Whole-field residuals were checked to ensure that the converged solution set satisfies the governing equations within a prescribed error.

Due to the large number of cases studied it was not possible to check the grid independence for each individual case. To overcome this problem, as suggested by Hosseinalipour and Mujumdar [12], the appropriate number of grids were found through a grid doubling procedure for the "worst" case with the highest Reynolds number for each geometry and applied to all other cases for that particular geometry. This procedure results in longer running times for the lower Reynolds number cases but it was compensated for by the time saving in not running grid doubling runs for each individual case. For details regarding the discretization of the governing equations and various schemes used to solve the discretized equations the reader may refer to Patankar [18].

The above model was verified by comparison with the experimental and numerical results of Roy et al. [15] who studied mixing flow in a junction (one-way exit impinging streams). This junction configuration is shown schematically in Fig. 2; the symmetrical plane in Fig. 1 is replaced by a solid wall in this case. The width of the inlet channels is half the exit channel height. All walls were specified to be adiabatic (well insulated).

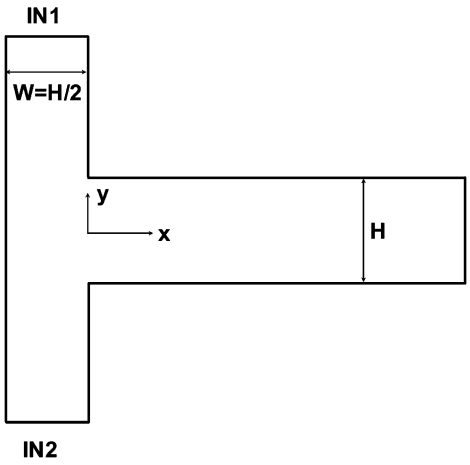

Fig. 2. Schematic diagram of the junction used in model verification.

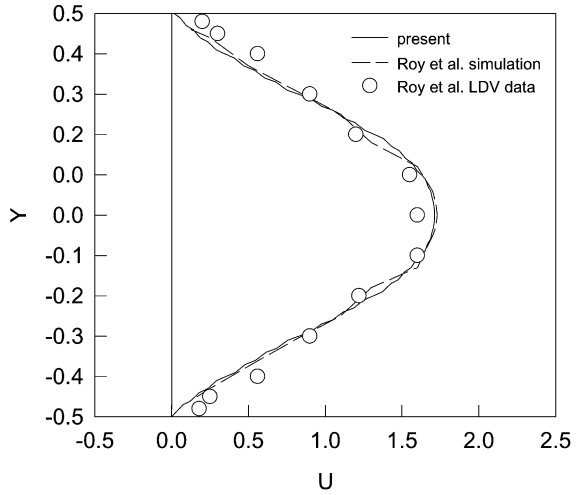

Fig. 3. Comparison of dimensionless axial velocity profiles. $Re = U_0 H\rho/\mu = 500$ (based on the mean velocity in the exit branch); $X = x/H = 5$ (where H is the height of the exit branch, see Fig. 2); $Y = y/H$, $U = u/U_0$, where U_0 is the mean velocity in the exit branch.

Fig. 3 compares the predicted dimensionless axial velocity profiles using the present simulation with both the numerical and experimental results of Roy et al. [15]. It is seen from this figure that the present results are in good agreement with both sets of data. The small discrepancies may be due to the slight differences in the measuring positions used in the experiment and the simulation. No data are available for temperature fields in similar configurations.

3. Results and discussion

Fluid (air in this case) was injected into the system through the two inlets (see Fig. 1). The two streams impinged normally against each other and then left the system through the exit channels situated symmetrically on either side of the impingement region. The length of the mixing channel was extended long enough to satisfy the fully developed channel flow assumption. To study mixing of the two fluid streams air of different temperatures was injected through each inlet channel. The ranges of parameters studied are: inlet jet Reynolds number (Re_j) from 500 to 10 000 for time-dependent cases and from 10 to 3500 for steady cases; the ratio of the height of the exit channel to the width of the inlet jet (H/W) was varied from 1.0 to 4.0.

By solving the transient conservation equations for mass, momentum and energy it was possible to obtain conditions where the flow begins to shift from laminar to a transitional and then a random flow regime. The velocity components were sampled at each time step at $x = W/2$ and $y = 0$ to determine if the flow was unsteady (either periodic or random oscillatory). These results are shown in Fig. 4. This figure shows that the transition Reynolds number depends strongly on the geometric configuration, viz. H/W, especially at lower

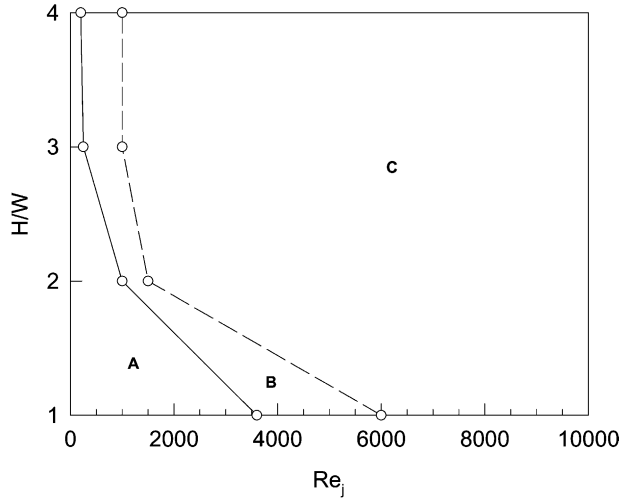

Fig. 4. Flow regime diagram: (A) stable; (B) oscillatory (periodic); (C) random oscillatory.

values of H/W. A similar study has been reported by Roy et al. [15] for the transition Reynolds number of the flow in a junction (one-way impinging streams). Only one case with $H/W = 2$ is reported in their study, however. They mentioned that the flow in the exit branch becomes turbulent for $Re > 500$ (based on the mean velocity in the exit branch). Using the present computer code the transition Reynolds number is identified to be $Re \approx 700$. The discrepancy between our numerical and their experimental results may be due to the presence of unavoidable disturbances when conducting the real experiment, which may lead to an earlier onset of instability than the one obtained numerically. Similar trend has been reported by Wood et al. [10] who studied experimentally and numerically the flow field created by two impinging liquid jets in a cylindrical chamber. They found that the calculations are more stable than the experimental conditions with respect to stability of the flow. This is due to the fact that the computational inlet boundary condition is fixed properly while in the experiments a pressure wave would be fed back into the jet itself, which could create a disturbance and promote oscillations in the mixing chamber. Nevertheless, this shows that the code performs quite satisfactorily in predicting the flow characteristics of impinging streams.

Some typical plots of the velocity component in the y-direction are shown in Figs. 5 and 6, where various oscillating and fluctuating patterns can be identified. Similar behavior is observed for each case for the velocity component in the x-direction as well. It can be seen in these figures that the oscillations as well as fluctuations diminish

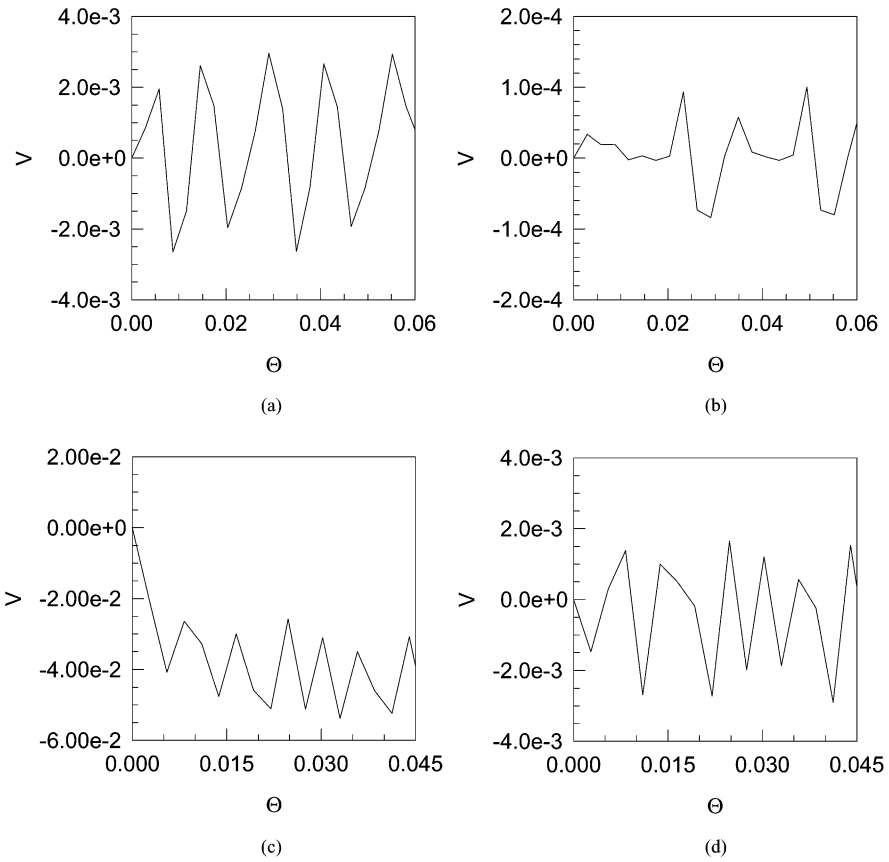

Fig. 5. Some oscillating patterns of velocity component in y-direction: (a) $H/W = 1.0$, $x/(W/2) = 1.0$, $Re_j = 4000$; (b) $H/W = 1.0$, $x/(W/2) = 50$, $Re_j = 4000$; (c) $H/W = 3.0$, $x/(W/2) = 1.0$, $Re_j = 500$; (d) $H/W = 3.0$, $x/(W/2) = 50$, $Re_j = 500$.

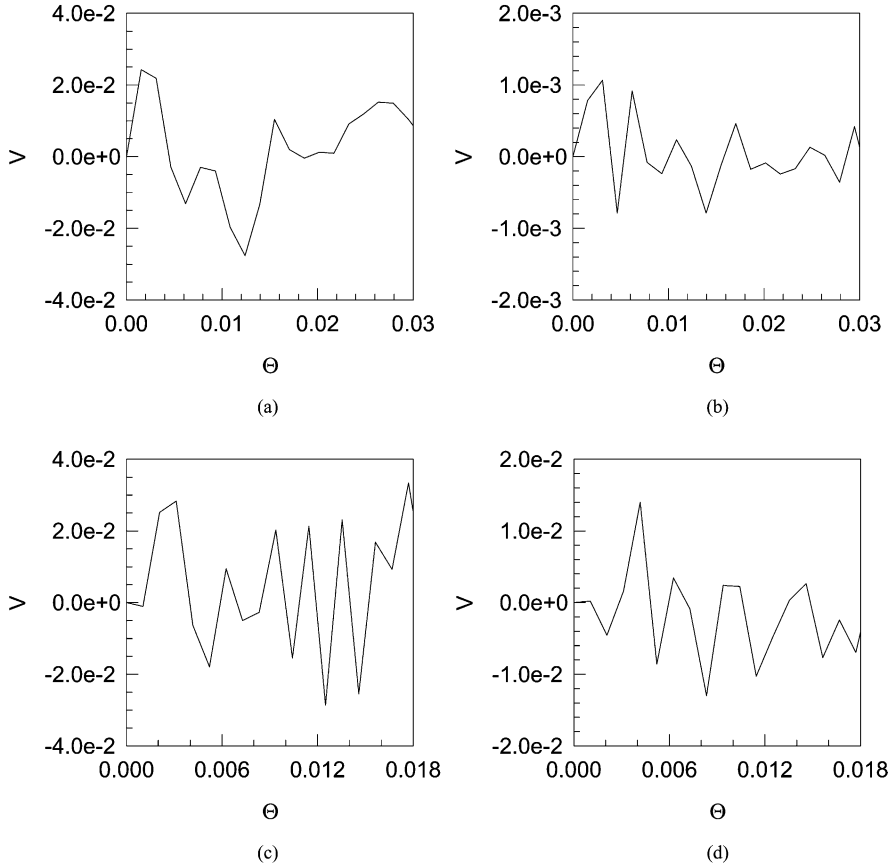

Fig. 6. Some fluctuating patterns of velocity component in *y*-direction: (a) $H/W = 1.0$, $x/(W/2) = 1.0$, $Re_j = 7500$; (b) $H/W = 1.0$, $x/(W/2) = 50$, $Re_j = 7500$; (c) $H/W = 2.0$, $x/(W/2) = 1.0$, $Re_j = 3000$; (d) $H/W = 2.0$, $x/(W/2) = 50$, $Re_j = 3000$.

as the exit ports are approached. It is seen in Fig. 5 that the degree of oscillation (amplitude as well as frequency of oscillation) is smaller at lower *H*/*W* despite the higher value of Re_j; the further away from the stable regime the higher is the degree of oscillation. Similar trend is observed for the fluctuating cases shown in Fig. 6. The diminishing of the fluctuating velocity component is not as clear as can be seen for the oscillating cases, however.

As noted earlier temperature was used as a passive tracer to study mixing of the two fluid streams introduced into the system. As the two streams mix and approach the exit ports the temperature profiles across the exit channel height are flattened; the well-mixed condition is satisfied when no temperature gradient exists across the channel height, i.e. the temperature profile is flat. To study the mixing performance of the system at different operating conditions and geometric configurations a mixing index was defined as follows:

$$\text{Mixing index} = \frac{\sigma_T}{\Delta T} \tag{11}$$

where σ_T is the standard deviation of the fluid temperature across the channel height at any specific axial location and ΔT is the temperature difference of the two inlet streams. $\sigma_T = 0$ thus implies well-mixed condition. Note that different criteria for mixing (e.g. the one proposed by Hosseinalipour and Mujumdar [12]) may be used but the above criterion is conceptually easier to visualize. Nonetheless, either index should equally predict the channel length required to well mix the two streams.

As mentioned earlier simulations were performed for cases with inlet jet Reynolds numbers in the stable regime to study the mixing characteristics of the system. The plots of velocity vectors and temperature isotherms of two representative cases are shown in Fig. 7. At low *H*/*W*, i.e. $H/W = 1$, no recirculating bubble is observed at low Re_j (say $Re_j < 1000$). The flow develops only a short distance downstream of the impingement region. The jet interaction is also weak; the two jets seem to flow parallel to and do not penetrate into each other even in the zone of impingement. This trend continues to hold even at higher Re_j, i.e. $Re_j = 3500$. As *H*/*W* increases recirculating bubbles are observed at much lower Re_j. The vortices size increases with increased Re_j; this trend is more pronounced at higher values of *H*/*W*. The jet interaction is also stronger as *H*/*W* increases as is seen in Fig. 7b. A structure similar to the "pancake" reported by Wood et al. [10] can also be seen in this figure. The flow develops much later downstream compared to the case shown in Fig. 7a. Large recircu-

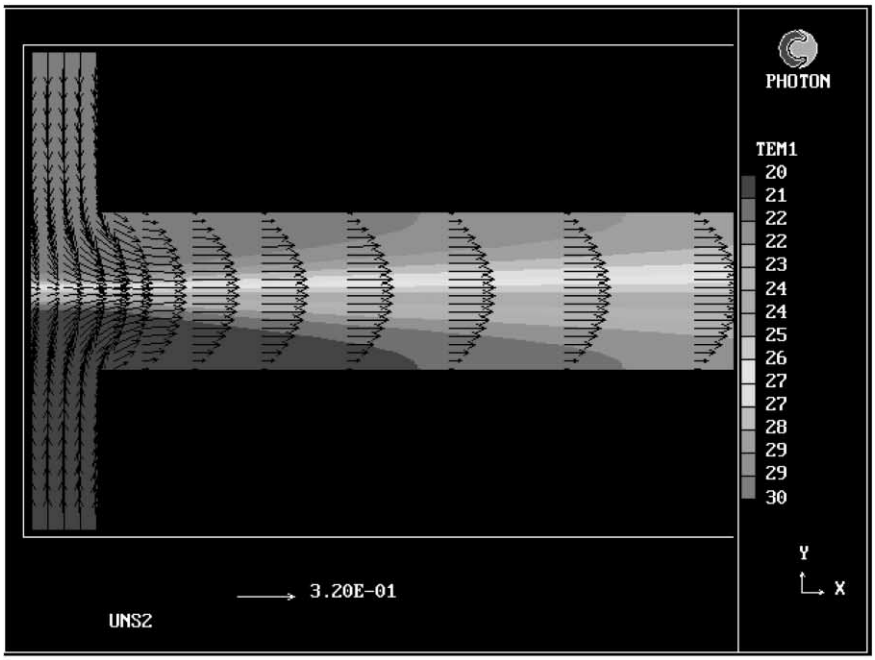

(a)

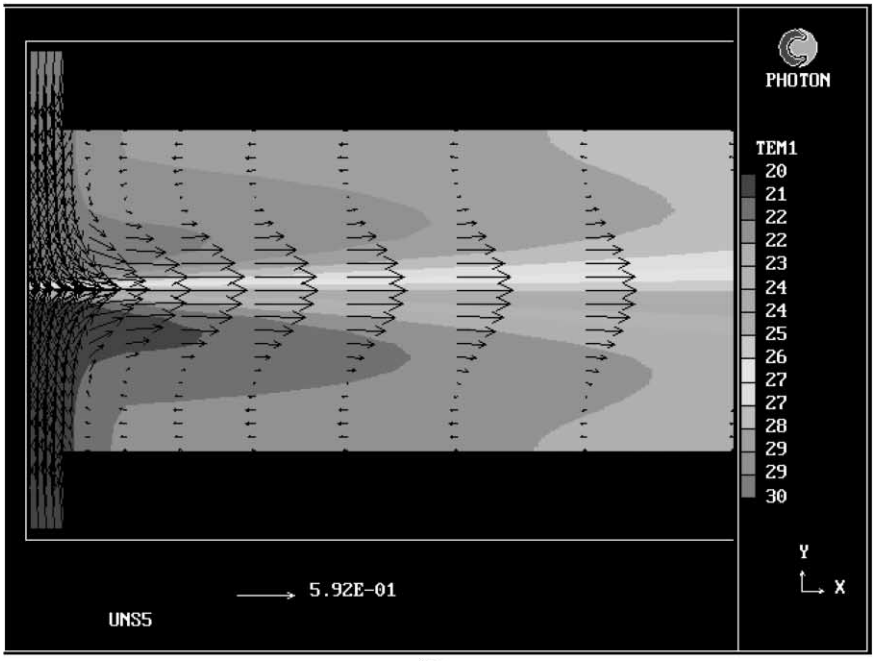

(b)

Fig. 7. (a) Velocity vectors and temperature contours $H/W = 1.0$, $Re_j = 200$; (b) velocity vectors and temperature contours $H/W = 4.0$, $Re_j = 200$.

lating bubbles are also seen in this figure. The shape of the temperature profiles is affected by the jet interaction and the presence of the vortices as can be seen in this figure.

The plots of the mixing index versus dimensionless axial distance with the jet Reynolds number as a parameter are shown in Fig. 8a–d for $H/W = 1$–4, respectively. Both dimensional and dimensionless coordinates are shown in these figures for easy comparison. It should be noted that the upper limit of $x/(W/2) = 200$ in these figures was chosen arbitrarily and does not imply that the computational domain ends at that particular value. The fully developed assumption at the exit still holds for all cases reported here.

It can be seen from these figures that a longer exit channel is required for complete mixing as the jet Reynolds

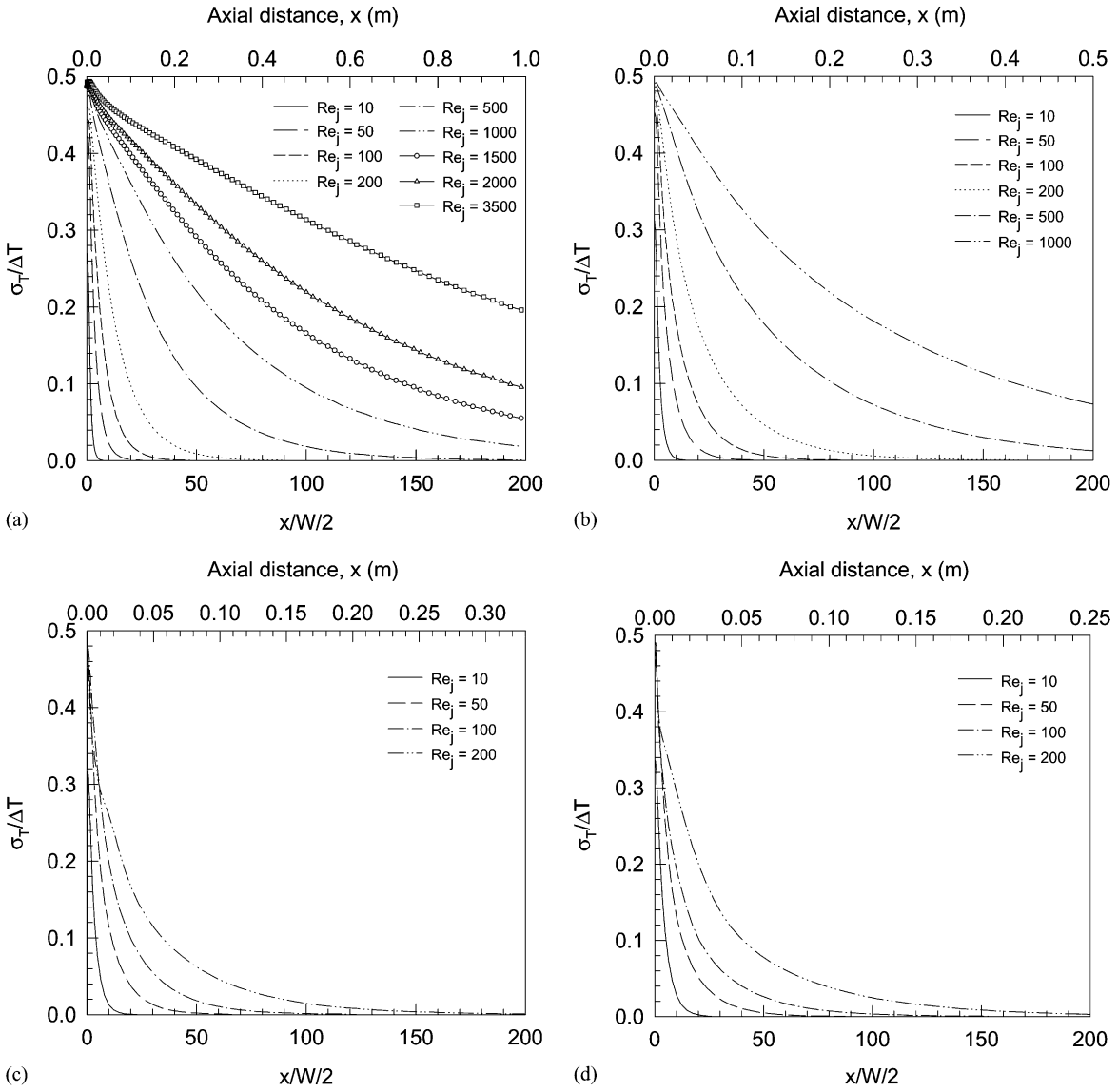

Fig. 8. (a) Mixing index for $H/W = 1.0$; (b) mixing index for $H/W = 2.0$; (c) mixing index for $H/W = 3.0$; (d) mixing index for $H/W = 4.0$.

number increases. This trend holds for all *H*/*W* studied. This may be ascribed to the increase in momentum of the fluid in the exit channel (and hence shorter residence time of the fluid in the system) due to the additional mass coming into the system. At low *H*/*W*, i.e. $H/W = 1$–2, the mixing curves scale monotonically with Re_j since very small jet interaction occurs. Thermal mixing is mainly by diffusion. As *H*/*W* increases the jet interaction is stronger and hence a better mixing in the impingement zone and its vicinity. For a particular value of the jet Reynolds number the distance to attain well-mixed condition increases in the dimensionless distance but decreases dimensionally with *H*/*W* since the transverse diffusive term in the energy equation becomes less dominant as *H*/*W* increases. Very good mixing is obtained over a rather short distance for all cases studied, however.

Fig. 9 shows the plots of the mixing index versus *x*/(*W*/2) with *H*/*W* as a parameter. The upper limit of $Re_j = 200$ was chosen here since this is the last point where a laminar steady solution can be obtained for $H/W = 4$ (see Fig. 4). Again, as *H*/*W* increases the dimensionless length of the exit channel required to well mix the two streams increases. This effect of *H*/*W* on the mixing length, however, decreases with an increase in *H*/*W*. The effect of the jet interaction on the mixing in the impingement region can be seen again in Fig. 9c and d. As *H*/*W* increases the jet interaction is stronger and hence a better mixing (Fig. 9c). As *H*/*W* becomes higher and hence the higher jet velocity at the same Re_j due to the smaller jet opening the higher lateral momentum tends to push the fluid out the system faster. This leads to a poorer mixing at high Re_j and *H*/*W* as is seen in Fig. 9d.

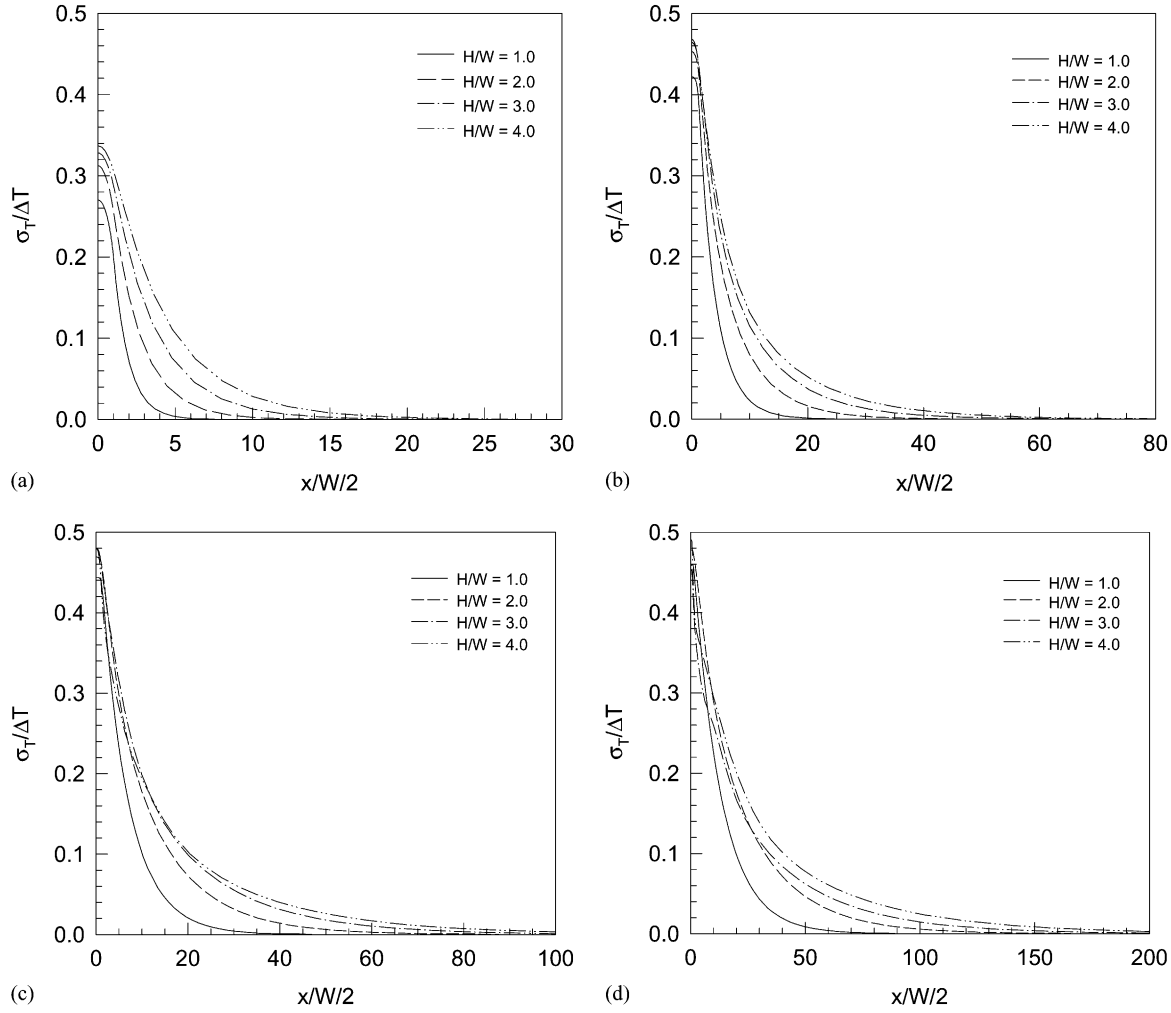

Fig. 9. (a) Mixing index for $Re_j = 10$; (b) mixing index for $Re_j = 50$; (c) mixing index for $Re_j = 100$; (d) mixing index for $Re_j = 200$.

4. Concluding remarks

Numerical simulations are reported on the flow and mixing characteristics of two-dimensional laminar confined impinging streams. Time-dependent conservation equations for mass, momentum and energy were solved to determine the condition when the flow starts to shift from laminar to transitional to random oscillatory flow regimes for various geometric configurations. Once the flow regime diagram has been established simulations were performed for cases in which steady-state solutions are obtainable to study the mixing characteristics of impinging streams. It is found that, for each geometric configuration, a longer exit channel is required to obtain well-mixed condition as the inlet jet Reynolds number increases. For the same inlet jet Reynolds number, it is found that the distance to attain the well-mixed condition increases dimensionlessly but decreases dimensionally with H/W. Very good mixing is obtained over a rather short distance for all cases examined. This confirms the benefits of using impinging streams in the mixing operation. The results presented here are useful for the preliminary design of an in-line mixer for high viscosity fluids utilizing a novel multiple impinging stream geometry.

References

[1] A. Tamir, Processes and phenomena in impinging-stream reactors, Chem. Eng. Progr. 85 (1989) 53–61.

[2] T. Kudra, A.S. Mujumdar, Impingement stream dryers for particles and pastes, Drying Technol. 7 (1989) 219–266.

[3] A. Tamir, Impinging-Stream Reactors: Fundamentals and Applications, Elsevier, Amsterdam, 1994.

[4] S.M. Hosseinalipour, A.S. Mujumdar, Flow, heat transfer and particle drying characteristics in confined opposing jets: a numerical study, Drying Technol. 13 (1995) 753–781.

[5] Y. Berman, A. Tamir, Experimental investigation of phosphate dust collection in impinging streams, Can. J. Chem. Eng. 74 (1996) 817–821.

[6] Y. Berman, A. Tanklevsky, Y. Oren, A. Tamir, Modeling and experimental studies of SO_2 absorption in coaxial cylinders with impinging streams: Part I, Chem. Eng. Sci. 55 (2000) 1009–1021.

[7] Y. Berman, A. Tanklevsky, Y. Oren, A. Tamir, Modeling and experimental studies of SO_2 absorption in coaxial cylinders with impinging streams: Part II, Chem. Eng. Sci. 55 (2000) 1023–1028.
[8] B. Yao, Y. Berman, A. Tamir, Evaporative cooling of air in impinging streams, AIChE J. 41 (1995) 1667–1675.
[9] D.R. Unger, F.J. Muzzio, R.S. Brodkey, Experimental and numerical characterization of viscous flow and mixing in an impinging jet contactor, Can. J. Chem. Eng. 76 (1998) 546–555.
[10] P. Wood, A. Hrymak, R. Yeo, D. Johnson, A. Tyagi, Experimental and computational studies of the fluid mechanics in an opposed jet mixing head, Phys. Fluids A 3 (1991) 1362–1368.
[11] D.A. Johnson, P.E. Wood, Self-sustaining oscillations in opposed impinging jets in an enclosure, Can. J. Chem. Eng. 78 (2000) 867–875.
[12] S.M. Hosseinalipour, A.S. Mujumdar, Flow and thermal characteristics of steady two-dimensional confined laminar opposing jets: Part I. Equal jets, Int. Comm. Heat Mass Transfer 24 (1997) 27–38.
[13] S.M. Hosseinalipour, A.S. Mujumdar, Flow and thermal characteristics of steady two-dimensional confined laminar opposing jets: Part II. Unequal jets, Int. Comm. Heat Mass Transfer 24 (1997) 39–50.
[14] E. Baydar, Confined impinging air jet at low Reynolds numbers, Exp. Thermal Fluid Sci. 19 (1999) 27–33.
[15] J.C. Roy, C. Bertrand, G. Le Palec, Numerical and experimental study of mixed and forced convection in a junction, Int. J. Heat Mass Transfer 37 (1994) 1985–2006.
[16] R.B. Bird, W.E. Stewart, E.N. Lightfoot, Transport Phenomena, Wiley, New York, 1960.
[17] Concentration, Heat and Momentum Limited (CHAM), POLIS: Phoenics On-line Information System, London, 1997, http://www.cham.co.uk.
[18] S.V. Patankar, Numerical Heat Transfer and Fluid Flow, Hemisphere, Washington, 1980.